PHYSICAL REVIEW E **66**, 050301(R) (2002)

Symmetry breaking and coarsening of clusters in a prototypical driven granular gas

Eli Livne,[1] Baruch Meerson,[1] and Pavel V. Sasorov[2]
[1]*Racah Institute of Physics, Hebrew University of Jerusalem, Jerusalem 91904, Israel*
[2]*Institute of Theoretical and Experimental Physics, Moscow 117259, Russia*
(Received 12 April 2002; published 19 November 2002)

Granular hydrodynamics predicts symmetry-breaking instability in a two-dimensional ensemble of nearly elastically colliding smooth hard disks driven, at zero gravity, by a rapidly vibrating sidewall. Supercritical and subcritical symmetry-breaking bifurcations of the stripe state are identified, and the supercritical bifurcation curve is computed. The cluster dynamics proceed as a coarsening process mediated by the gas phase. Well above the bifurcation point the final steady state, selected by coarsening, represents a single strongly localized densely packed ''droplet.''

DOI: 10.1103/PhysRevE.66.050301 PACS number(s): 45.70.Qj

I. INTRODUCTION

Rapid granular flow (RGF) continues to attract a great deal of attention from physicists [1]. Among the most fascinating phenomena in RGF is clustering: nucleation and growth of dense clusters of particles, surrounded by dilute granular gas in ''freely cooling'' [2] and driven [3–7] granular gases. Clustering phenomena can be viewed as a variant of thermal condensation instability, encountered also in gases and plasmas that cool by their own radiation [8]. This analogy brings about the question of universality of structure formation in ensembles of particles with energy losses of different natures. A related, albeit largely unexplored issue is *coarsening*. When reviewing different cluster-forming (and phase-separating) granular systems with a fixed number of particles [2,7,9], one notices that coarsening is ubiquitous. In many of these systems a *single* cluster survives after transients die out. The present work addresses different issues of phase separation and coarsening in driven granular gases. We consider a simple model system: an ensemble of inelastic hard spheres, confined in a rectangular box and driven by a rapidly vibrating side wall at zero gravity. Though this and related systems were investigated theoretically [3,4,10,11] and experimentally [6,12], it has only recently been recognized that they exhibit phase separation properties [13–15]. These properties will be in the focus of the present work. We shall employ granular hydrodynamics to predict the character of symmetry-breaking bifurcations of the stripe state and show that, depending on the control parameters, both supercritical and subcritical bifurcations can occur. We shall see that the selection of the final phase-separated state occurs via cluster coarsening mediated by the gas phase. Only one densely packed ''droplet'' survives far above the bifurcation point. These results give evidence that selection by coarsening is universal in cluster-forming granular flows with a fixed number of particles.

II. MODEL

Let $N \gg 1$ identical hard disks of diameter d and mass $m=1$ slide without friction on a smooth horizontal surface of a rectangular box with dimensions $L_x \times L_y$. The local number density of grains is n, the granular temperature is T. For a submonolayer coverage n is less than the (hexagonal) close-packing density $n_c = 2/(\sqrt{3}d^2)$. Three of the walls are immobile, and grain collisions with them are assumed elastic. The fourth wall (located at $x=L_x$) vibrates rapidly, $x = L_x + A\cos\omega t$, and supplies energy to the particles. The energy is lost via inelastic hard-core grain collisions, characterized by a constant coefficient of normal restitution r. In the quasi-elastic limit $1-r^2 \ll 1$ and for small Knudsen numbers, the Navier-Stokes granular hydrodynamics is expected to be reasonably accurate, even for large granular densities, as long as the granulate is fluidized [4]. Therefore, the steady states of the system are describable by the momentum and energy balance equations

$$p = \text{const}, \quad \boldsymbol{\nabla}\cdot(\kappa\boldsymbol{\nabla}T) = I, \tag{1}$$

where p is the pressure, κ is the thermal conductivity and I is the rate of energy losses. To make full use of hydrodynamics, we shall work in the parameter regime where the energy supply from the vibrating wall can be represented as a hydrodynamic heat flux. This requires $A \ll l_w$, where l_w is the mean free path of the particles at the vibrating wall. A double inequality

$$T_w^{1/2}/l_w \ll \omega \ll T_w^{1/2}/A \tag{2}$$

is also assumed (index w refers to the vibrating wall). The left inequality guarantees the absence of correlations between successive collisions of particles with the vibrating wall, while the right inequality simplifies the calculations, but is not crucial. (As T_w and l_w are determined by the parameters of the problem, criteria (2) should be *verified* [16].) The resulting energy flux is [13,17]

$$q = \kappa\partial T/\partial x = (2/\pi)^{1/2}A^2\omega^2 n_w T_w^{1/2}. \tag{3}$$

To make the hydrodynamic model closed, one needs constitutive relations (CRs): p, κ and I in terms of n and T. The CRs are derivable systematically only in the dilute limit. Reasonably accurate CRs in the whole range of densities can be obtained by employing free volume arguments close to the dense-packing limit, interpolating between the high- and low-density limits and finding the fitting constants by comparing the results with particle simulations [4,18]. We shall

use the CRs suggested by Grossman *et al.* [4] because of their relative simplicity. A special investigation [15] showed that the stability diagrams do not change much if one uses instead the CRs derived by Jenkins and Richman [19].

Eqs. (1) can be rewritten in terms of one variable: the (scaled) inverse density $z(x,y)=n_c/n(x,y)$ [4,13]. In the scaled coordinates $\mathbf{r}/L_x \to \mathbf{r}$ the box dimensions become $1 \times \Delta$, where $\Delta = L_y/L_x$ is the box aspect ratio. We obtain $\boldsymbol{\nabla}\cdot[F(z)\nabla z] = \mathcal{L}Q(z)$. Introducing $\psi = \int_0^z F(z')dz'$, we rewrite it as

$$\nabla^2 \psi = \mathcal{L}\tilde{Q}(\psi). \tag{4}$$

The boundary conditions are

$$\left.\frac{\partial\psi}{\partial x}\right|_{x=0} = \left.\frac{\partial\psi}{\partial y}\right|_{y=0} = \left.\frac{\partial\psi}{\partial y}\right|_{y=\Delta} = 0, \tag{5}$$

and (see Ref. [13])

$$\left.\frac{\partial\psi}{\partial x}\right|_{x=1} = \mathcal{L}\tilde{H}[\psi(1,y)]\frac{\int_0^\Delta\int_0^1 \tilde{Q}(\psi)\,dxdy}{\int_0^\Delta \tilde{H}(\psi(1,y))dy}. \tag{6}$$

Here $\tilde{Q}(\psi)=Q[z(\psi)]$ and $\tilde{H}(\psi)=H[z(\psi)]$, while F,G,H, and Q are functions of z only; they are presented in Ref. [13]. In the rest of the paper the symbol $\tilde{}$ will be omitted. The total number of particles is conserved,

$$\frac{1}{\Delta}\int_0^\Delta\int_0^1 \frac{dx\,dy}{z(\psi)} = \frac{N}{L_x L_y n_c} \equiv f. \tag{7}$$

The steady state problem is fully determined by three scaled parameters: $\mathcal{L}=(32/3\gamma)(L_x/d)^2(1-r^2)$ (where $\gamma \simeq 2.26$), the area fraction f and aspect ratio Δ.

III. STRIPE STATE

The basic state of the system is the stripe state: a laterally symmetric stripe of enhanced density, located at the wall $x=0$ [4]. The stripe state is described by the y-independent solution of Eqs. (4) and (5); we shall call it as $z=Z(x)$ corresponding to $\psi=\Psi(x)$. Notice that Eq. (6) automatically holds in one dimension (1D) [13]. An example of the stripe state is shown in Fig. 2 (bottom left).

IV. SYMMETRY-BREAKING INSTABILITY

The stripe state gives way, by a symmetry-breaking bifurcation, to 2D steady states. The bifurcation point can be found by linearizing Eqs. (4)–(7) around $\psi=\Psi(x)$. In the framework of *time-dependent* hydrodynamics, this corresponds to *marginal stability* of the stripe state with respect to small perturbations along the stripe. We write

$$\psi(x,y) = \Psi(x) + \varphi_k(x)\exp(iky) + \text{c.c.} \tag{8}$$

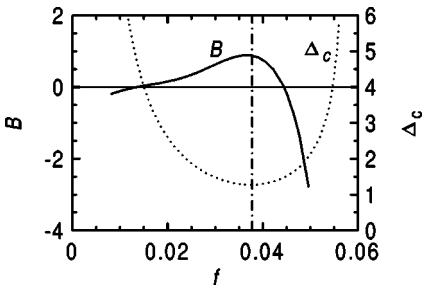

FIG. 1. The critical aspect ratio Δ for the instability and parameter B determining the bifurcation curve (20) versus the area fraction f for $\mathcal{L}=1.25\times10^4$. The vertical dash-dot line corresponds to $f=0.0378$.

and, after linearization, arrive at a linear eigenvalue problem for $k=k_c(f)$,

$$\varphi_k'' - \mathcal{L}Q_\Psi\varphi_k - k_c^2\varphi_k = 0, \tag{9}$$

$$\varphi_k'(0) = 0, \tag{10}$$

$$\varphi_k'(1) - \mathcal{L}\frac{\int_0^1 \tilde{Q}[\Psi(x)]dx}{\tilde{H}[\Psi(1)]}H_\Psi|_{x=1}\varphi_k(1) = 0. \tag{11}$$

Here and below $(\cdots)_\Psi(x) = [F^{-1}d(\cdots)/dz]|_{z=Z(x)}$, and $(\cdots)$ stands for any function. The eigenvalue problem was considered in different limits, and for different boundary conditions at the driving wall, in Refs. [13–15]. For a given $\mathcal{L}$, one obtains the marginal stability curve $k=k_c(f)$ and corresponding eigenfunctions $\varphi_k(x)$. The modes with $k<k_c(f)$ are unstable. At large enough $\mathcal{L}$, the instability occurs for $f_1(\mathcal{L})<f<f_2(\mathcal{L})$, where $k_c(f_1)=k_c(f_2)=0$ [13]. The driving force of the instability is negative effective lateral compressibility of the gas [15]. Figure 1 gives an example of the marginal stability curve in terms of the minimum aspect ratio $\Delta_c(f)=\pi/k_c(f)$ at which the instability occurs.

V. BIFURCATION CURVE

To determine the nature of the bifurcation (sub-critical or supercritical) and compute the bifurcation curve, one should go to the second order of the perturbation theory. We can write

$$\psi(x,y) = \Psi(x) + \sum_n \varphi_n(x)\exp(inky), \tag{12}$$

where $\varphi_{-n}(x)=\varphi_n^*(x)$, and assume that $\varphi_0 \sim \varphi_1^2$, $\varphi_2 \sim \varphi_1^2$, $\varphi_3 \sim \varphi_1^3$, etc. Therefore, it is only necessary to take into account the terms $n=0,\pm1$, and ±2, yielding the following linear equations:

$$\varphi_0'' - \mathcal{L}Q_\Psi\varphi_0 = \mathcal{L}Q_{\Psi\Psi}|\varphi|^2, \tag{13}$$

$$\varphi_1'' - \mathcal{L}Q_\Psi\varphi_1 - k_c^2\varphi_1 = (k^2-k_c^2)\varphi + \mathcal{L}[Q_{\Psi\Psi}(\varphi_0\varphi+\varphi_2\varphi^*) + \tfrac{1}{2}Q_{\Psi\Psi\Psi}\varphi|\varphi|^2], \tag{14}$$

$$\varphi_2'' - \mathcal{L} Q_\Psi \varphi_2 - 4k_c^2 \varphi_2 = \frac{1}{2} \mathcal{L} Q_{\Psi\Psi} \varphi^2, \tag{15}$$

and the boundary conditions:

$$\varphi_0'(0) = \varphi_1'(0) = \varphi_2'(0) = 0, \tag{16}$$

$$\varphi_2'(1) = \mathcal{L}\left[\frac{H_\Psi}{H}\varphi_2 + \frac{H_{\Psi\Psi}}{2H}|\varphi|^2\right]\Bigg|_{x=1} \int_0^1 Q dx, \tag{17}$$

where $\varphi = A\,Y(x)$ is a properly normalized solution of Eqs. (9)–(11) (see below). A cumbersome but straightforward boundary condition for φ_1 at $x=1$ is not presented here, please see Ref. [20]. As the boundary condition for φ_0 at $x=1$ is fulfilled automatically, one more condition is needed which is supplied by Eq. (7),

$$\int_0^1 \frac{\varphi_0}{Z^2 F} dx = 2\int_0^1 \left(\frac{1}{Z^3 F^2} + \frac{F_\Psi}{2Z^2 F^2}\right)|\varphi_1|^2 dx. \tag{18}$$

The solvability condition for Eqs. (13)–(15) yields the bifurcation curve: a relation between the amplitude of φ_1 (we call it A) and $k_c^2 - k^2$. One way to define A is the following: $\varphi_1(x) = A\,Y(x) + A|A|^2\,\delta\varphi_1(x)$, where $Y(x)$ is the solution of Eqs. (9) and (10) such that $Y(0)=1$. This yields $A(k_c^2 - k^2) = CA|A|^2$, where $C=$const. The trivial solution $A=0$ describes the stripe state, while the nontrivial one, $k_c^2 - k^2 = C|A|^2$ describes the bifurcated state. $C>0$ (<0) corresponds to supercritical (subcritical) bifurcation. The solvability condition is a generalization of the standard ''orthogonality'' condition, or the Fredholm alternative [21]. It yields C explicitly in terms of definite integrals of solutions of the homogeneous forms of Eqs. (9), (13), and (15) that can be found numerically, see Ref. [20] for detail. We present here the resulting bifurcation curve for Y_c, the (normalized) y coordinate of the center of mass of the granulate,

$$Y_c = \frac{\int_0^1 dx \int_{-\Delta/2}^{\Delta/2} y z^{-1} dy}{\Delta \int_0^1 dx \int_{-\Delta/2}^{\Delta/2} z^{-1} dy}, \tag{19}$$

where we shifted the y coordinate $y + \Delta/2 \to y$. Let the aspect ratio of the system Δ be slightly larger than $\Delta_c = \pi/k_c(f)$ so that only one mode, with $k = \pi/\Delta$, is unstable. The bifurcation curve takes the form

$$|Y_c| = \frac{2}{\pi^2 B^{1/2}}\left(\frac{\Delta}{\Delta_c} - 1\right)^{1/2}, \tag{20}$$

where $B = Cf^2/(2k_c^2 f_1^2)$ and $f_1 = 2\int_0^1 Y Z^{-2} F^{-1} dx$. Equation (20) assumes $B>0$: a supercritical bifurcation. Figure 1 shows $B(f)$ for $\mathcal{L} = 12\,500$. We found that $B>0$ on an interval of f that lies *within* the instability interval (f_1, f_2). Closer to the points f_1 and f_2 we obtained $B<0$ which indicates subcritical bifurcation. Subcritical bifurcations close to the high-density instability border were previously observed by solving numerically the nonlinear steady state equations (4)–(6) [13].

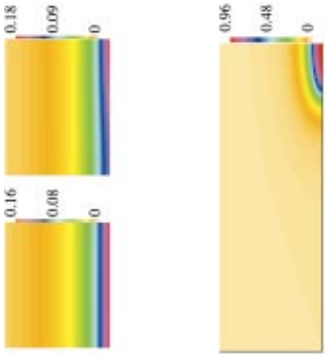

FIG. 2. (Color) Steady states found in time-dependent hydrodynamic simulations for $\mathcal{L} = 1.25\times 10^4$, $f = 0.0378$ and $\Delta = 1.2$ (bottom left), 1.3 (top left) and 3.0 (right). The left wall of the box is the driving wall.

VI. HYDRODYNAMIC SIMULATIONS: BIFURCATION AND COARSENING

We performed a series of hydrodynamic simulations, to verify the bifurcation theory and to follow the cluster dynamics at large aspect ratios. The full time-dependent hydrodynamic equations were solved with the same constitutive relations and boundary conditions as those used in our steady state analysis. Instead of the shear viscosity in the Navier-Stokes equation we accounted for a small model friction force $-n\mathbf{v}/\tau$, where $\mathbf{v}$ is the hydrodynamic velocity. An extended version of the compressible hydrocode VULCAN [22] was employed.

We set $\mathcal{L} = 1.25\times 10^4$ and $f = 0.0378$ and varied Δ. The initial scaled density included a zero mode corresponding to the fixed f plus small-amplitude random noise. Figure 2 shows the final states for different aspect ratios Δ. For $\mathcal{L}$ and f used, the marginal stability theory predicts $\Delta_c \simeq 1.28$ (see Fig. 1). Indeed, the stripe state observed at $\Delta = 1.2$ (Fig. 2, bottom left) gives way to a slightly asymmetric state at $\Delta = 1.3$ (Fig. 2, top left). Well above the bifurcation point, the final state represents a densely packed island, or droplet (Fig. 2, right). This implies that all but one of the multiple 2D steady state solutions found earlier (chains of islands periodic in the y direction) [13] are unstable. The stable steady state selected by the coarsening dynamics is the one with the maximum possible period. For the boundary conditions employed in this work, the maximum period is twice the lateral dimension of the system.

Figure 3 shows the bifurcation curve $Y_c(\Delta)$ predicted by Eq. (20), and measured in the simulations after transients die out. Excellent agreement is obtained for not too large supercriticalities. Close to the bifurcation point we observed exponential slowdown as expected.

Now we present the simulation results on the cluster dynamics and selection. For larger Δ the dynamics involve two stages (see Fig. 4). During the first stage, several clusters nucleate at the wall opposite to the driving wall. Their num-

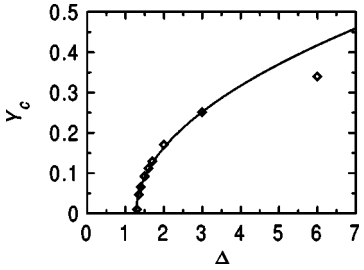

FIG. 3. Bifurcation curve $Y_c(\Delta)$ predicted by Eq. (20) (line) and found in hydrodynamic simulations (squares) for $\mathcal{L}=1.25\times10^4$ and $f=0.0378$.

ber is of the order of Δ/Δ_c, which apparently corresponds to the maximum linear growth rate of the instability versus k. At the slower second stage the clusters densify and, as they compete for material, their number decreases, and only one densely packed droplet finally survives. The clusters interact mostly through the gas phase, similarly to Ostwald ripening in phase-ordering systems with a conserved order parameter, controlled by gasdynamics [8,23]. A direct merger of transient clusters was also observed, for another realization of noise in the initial conditions. The resulting single droplet, however, was always the same in simulations with the same $\mathcal{L}$, f, and Δ.

VII. SUMMARY

In summary, we employed hydrodynamics to determine the character of symmetry-breaking bifurcations that lead to phase separation in a prototypical driven granular gas. The supercritical bifurcation curve was computed. We found that the selection of the phase-separated steady state is made via a coarsening process similar to Ostwald ripening. It appears that cluster selection by coarsening is a universal selection mechanism in cluster-forming granular flows with a fixed number of particles. We hope that this process will be observed in experiment with spherical particles rolling on a smooth surface [6,12].

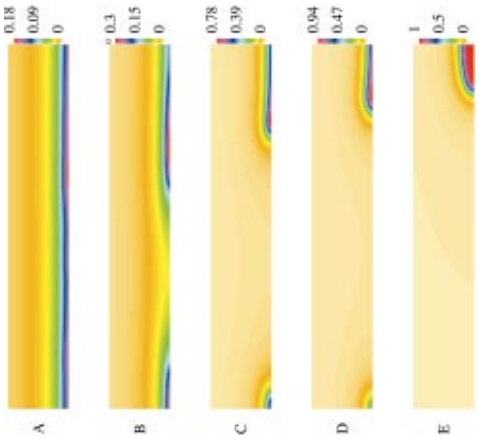

FIG. 4. (Color) Time history of the density field for $\mathcal{L}=1.25\times10^4$, $f=0.0378$, and $\Delta=5$ at scaled times 650 (A), 2,100 (B), 2,850 (C), 3,250 (D), and 7,000 (E). The left wall is the driving wall. Notice the change of color code with time.

ACKNOWLEDGMENTS

This research was supported by the Israel Science Foundation, founded by the Israel Academy of Sciences and Humanities, and by the Russian Foundation for Basic Research (Grant No. 02-01-00734).

[1] H.M. Jaeger, S.R. Nagel, and R.P. Behringer, Rev. Mod. Phys. **68**, 1259 (1996); L.P. Kadanoff, *ibid.* **71**, 435 (1999).
[2] M.A. Hopkins and M.Y. Louge, Phys. Fluids A **3**, 47 (1991); I. Goldhirsch and G. Zanetti, Phys. Rev. Lett. **70**, 1619 (1993); S. McNamara and W.R. Young, Phys. Rev. E **53**, 5089 (1996).
[3] Y. Du, H. Li, and L.P. Kadanoff, Phys. Rev. Lett. **74**, 1268 (1995).
[4] E.L. Grossman, T. Zhou, and E. Ben-Naim, Phys. Rev. E **55**, 4200 (1997).
[5] S.E. Esipov and T. Pöschel, J. Stat. Phys. **86**, 1385 (1997).
[6] A. Kudrolli, M. Wolpert, and J.P. Gollub, Phys. Rev. Lett. **78**, 1383 (1997).
[7] J.S. Olafsen and J.S. Urbach, Phys. Rev. Lett. **81**, 4369 (1998).
[8] B. Meerson, Rev. Mod. Phys. **68**, 215 (1996).
[9] I.S. Aranson *et al.*, Phys. Rev. Lett. **84**, 3306 (2000).
[10] J.J. Brey and D. Cubero, Phys. Rev. E **57**, 2019 (1998).
[11] J. Tobochnik, Phys. Rev. E **60**, 7137 (1999).
[12] A. Kudrolli and J. Henry, Phys. Rev. E **62**, R1489 (2000).
[13] E. Livne, B. Meerson, and P.V. Sasorov, Phys. Rev. E **65**, 021302 (2002); e-print cond-mat/0008301.
[14] J.J. Brey, M.J. Ruiz-Montero, F. Moreno, and R. García-Rojo, Phys. Rev. E **65**, 061302 (2002).
[15] E. Khain and B. Meerson, Phys. Rev. E **66**, 021306 (2002); e-print cond-mat/0201569.
[16] Let the gas at the vibrating wall be dilute. Assuming $f\sqrt{\mathcal{L}}\gtrsim1$ and using Eqs. (1) and (3), we obtain $n_w^{-1}\sim d(1-r)^{1/2}L_x$ and $T_w\sim A^2\omega^2(1-r)^{-1/2}$. Therefore, the left inequality in Eq. (2) requires $A\ll(1-r)^{3/4}L_x$. If this condition holds, then the condition $A\ll l_w$ also holds. The right inequality in Eq. (2) is obeyed automatically.
[17] V. Kumaran, Phys. Rev. E **57**, 5660 (1998).
[18] S. Luding, Phys. Rev. E **63**, 042201 (2001).
[19] J.T. Jenkins and M.W. Richman, Phys. Fluids **28**, 3485 (1985).
[20] E. Livne, B. Meerson, and P.V. Sasorov, e-print cond-mat/0204266.
[21] G. Iooss and D.D. Joseph, *Elementary Stability and Bifurcation Theory* (Springer, New York, 1980), p. 88.
[22] E. Livne, Astrophys. J. **412**, 634 (1993).
[23] I. Aranson, B. Meerson, and P.V. Sasorov, Phys. Rev. E **52**, 948 (1995).